Session U-04

EXPERIMENTAL AND NUMERICAL INVESTIGATIONS OF FLOW OVER A FLAPPING AIRFOIL

Edward W. Eaves, Ning Zhang
Department of Engineering
McNeese State University
Lake Charles, LA 70609
will@camtel.net; nzhang@mcneese.edu;

Abstract

The purpose of the study is to investigate the flow characteristics around flapping airfoil, aiming the design of the novel Micro-Aerial Vehicles (MAVs) which mimic the flying motion of birds and insects. The chief objectives of the effort are the fabrication of two test airfoils, flapping mechanism for the test airfoil in the wind tunnel test, and the analysis of the velocity fluctuations in the vicinity of the airfoil. The airfoil flapping is a combined heave and pitch motion, over a frequency range from 1 to 3Hz. A specially manufactured NACA0012 and 0015 airfoils were used in the experiments, and was pitched sinusoidally about one half chord between angles of attack -15^{o} and 15^{o}. Numerical simulations were also conducted to validate the experiment measurements. Particularly, the regions very close to the airfoils are scrutinized as simulation for the airflow around a bird's wing.

1. Introduction

Since the mid-1990's an increased interest in developing MAVs has been expressed by both civilian and military organizations[1]. The shape of a MAV is intended to craft the airflow along the surface to manufacture a lifting force in the most proficient method. In addition to the lift, a force completely divergent from the movement of the wing through the air is always there, which is called a drag force. The angle of attack (AoA) is the angle between the free-stream velocity and the chord line of the airfoil. These forces are shown below in Figure 1. These forces vary with the change of the attack angle. It is desirable for the airfoil to have the maximum lift and smallest possible drag.

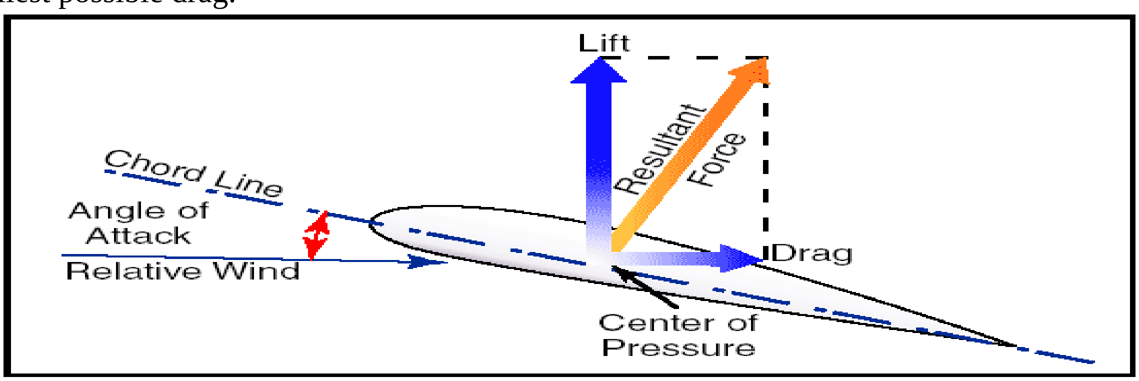

Figure 1, illustration of an airfoil[2]

2. Design Method

Figure 2 shown below is one of the airfoils fabricated at Dubois Sheet Metal Works in Lake Charles, La. The shape of the airfoils is similar to NACA 0015 airfoil. The airfoil is made from atomized aluminum to create enhanced fluid flow.

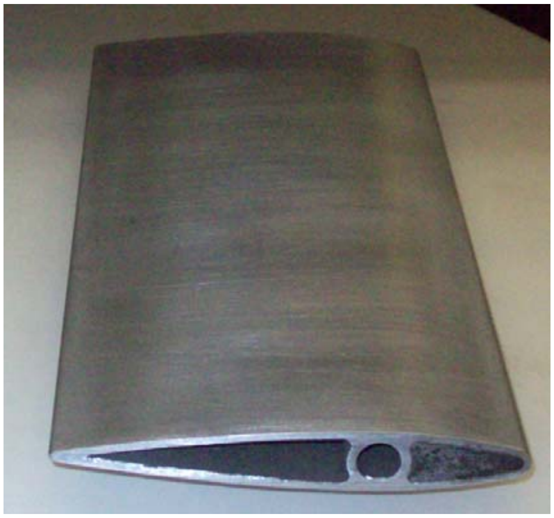

Figure 2, NACA 0015 airfoil

The experiment and the flapping mechanism for the wind-tunnel were designed around the following parameters: angle of attack, free-stream velocity, Reynolds number, and Strouhal number. The DC motor chosen for the experiment operates between 1-3 Hz. The angle of attack was chosen as 15 ^{o} and the other parameters were calculated using a program written in MatLab. The free-stream velocity, m/s, was determined using the following formula:

$$V = 0.9333 * fr - 1.2309 \qquad (1)$$

where *fr* is the frequency set on the control panel of the wind-tunnel. The Reynolds number for both airfoils was calculated using the following formula:

$$Re = \frac{V * c}{v} \qquad (2)$$

where c is the chord length of the airfoil, and v is the kinematic viscosity. Ohmi et al.[3] used a parameter called Strouhal number, the dimensionless flapping frequency of birds, as an important parameter governing the structure of the wake generated by a flapping foil:

$$St = \frac{f * c}{V} \qquad (3)$$

where f is the oscillation frequency of the motor driving the mechanism. Figure 3 shown below is the experimental setup with the 3-inch airfoil installed after fabrication. The mechanism is designed to give the predetermined angle of attack for both airfoils. The position, velocity, acceleration, and torque analysis was calculated as a four bar linkage for the mechanism design with 5-inch airfoil. The maximum acceleration and torque was found to be 26.67 $rad/_{s^2}$ and $4.81\ N*m$ respectively. This information was used to choose a DC gear-motor and controller made by Dayton that provided the necessary torque required. The linkage lengths were chosen because the longer the linkage the more stable the sinusoidal pitching motion of the airfoil. Shank bolts and brass bushings were used at the connections. The pulley was fabricated with keyway and two holes for the different airfoils. The different holes were needed for the mechanism to pitch at the prescribed angle of attack for each airfoil. The mechanism was fabricated at Hughes Welding and Fabrications in Jennings, La.

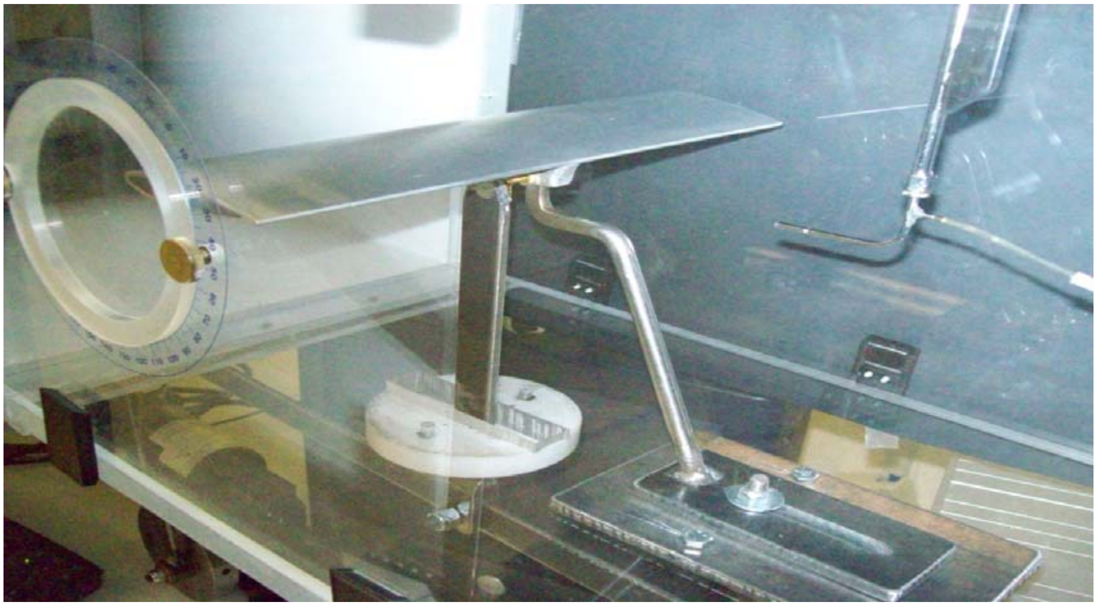

Figure 3, experimental setups

3. Results and Discussion

During the experiment, both stationary and flapping (pitching only) airfoil data were collected, along with a set of data without presence of the airfoil. The velocity was sampled 20 times per second that is small enough to resolve the flapping frequency. The duration of data collection was two minutes. For no airfoil and stationary airfoil cases, the data were collected at the location 1-chord length, which is 3 inches, behind the trailing edge of the airfoil. For flapping airfoil case, the following five locations were used for data collection in respect to trailing edge of the airfoil: (3in, -3in), (3in, -1.5in), (3in, 0in), (3in, 1.5in), and (3in, 3in). This data were used to create a velocity profile.

Figure 4 shows the velocity data collected from the experiments. For the quality of visualization, only the first minute data were shown. The Reynolds number for the experiment was about 40,000. The dimensionless oscillating frequency, the Strouhal number, was 0.1375. The pitching amplitude was 15^o. The wind-tunnel frequency was set at 10.1 Hz and the frequency of the gear-motor was set at 1.57 Hz. In Figure 4, at the same measurement location, the comparison has been made among 4 cases: a) without airfoil, which represents the free stream velocity in front of the airfoil; b) with airfoil of 0^o AoA; c) with airfoil of 15^o AoA; d) with flapping airfoil. Without the airfoil, the wind tunnel produced about 8m/s speed, and the turbulence intensity was about 7%. For the two stationary airfoil cases, the time-averaged velocity magnitudes were both smaller than the free stream velocity, which indicated the drag production due to the presence of the airfoil. Comparing between (b) and (c), 15^o AoA has smaller velocity magnitude, thus greater drag. For flapping case, the time-averaged velocity magnitude was increased which indicated lower drag. The time-averaged velocity magnitude comparison is shown in Figure 5. Another observation from Figure 4 is the velocity oscillation patterns are different between flapping airfoil and stationary airfoil cases. The spectrum analysis were performed and the results indicated that the dominant frequency of the flapping case was the flapping frequency while it was the natural vortex shedding frequency for the stationary airfoil cases.

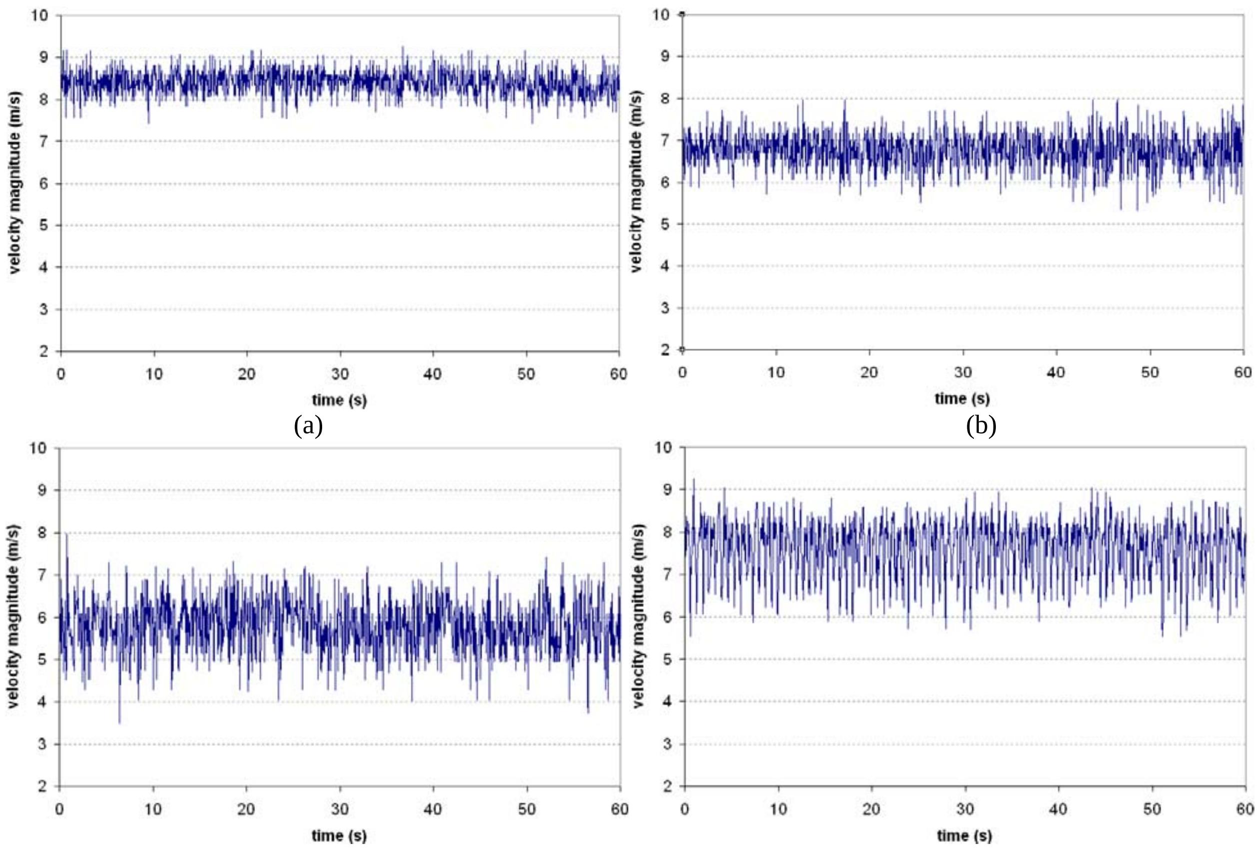

Figure 4 velocity magnitude history at the center of the test section, (a) without airfoil; (b) with stationary airfoil, 0^o AoA; (c) with stationary airfoil 15^o AoA; (d) with flapping (pitching) airfoil

Figure 6 shows the time-averaged velocity distribution on a vertical line at one chord length downstream of the trailing edge of the flapping airfoil. The comparison has been made between current experimental measurement and CFD simulation results. The simulation was performed using the immersed-boundary method[4] for the case of Re=1000 and with pitching only flapping motion. Figure 5 shows reasonably good agreement comparing to simulation data. The shapes of two curves match for the top half of the profile, but the measured data are smaller than the simulation prediction for the bottom half of the profile. The problem with the profile was determined to be the presence of the ground link supporting the airfoil, shown in Figure 3. The airflow underneath the airfoil was partially blocked thus caused the lower velocity in the bottom half of the test section.

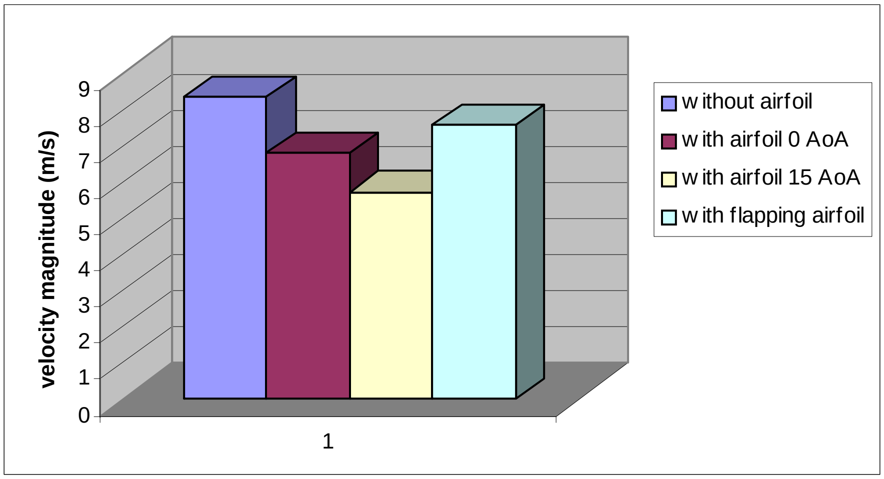

Figure 5 the time-averaged velocity-magnitude comparison

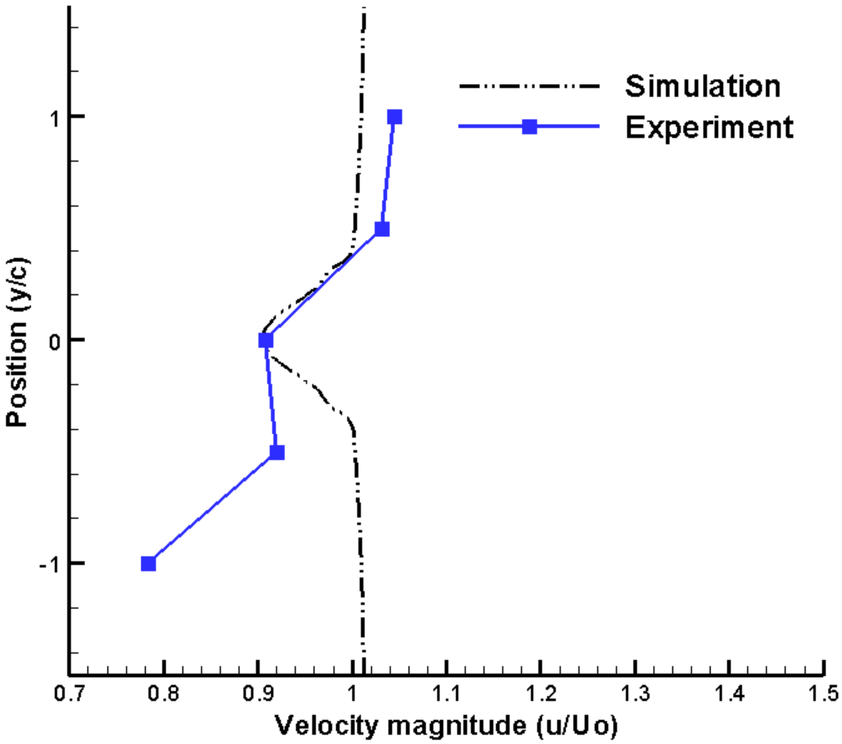

Figure 6, time-averaged velocity magnitude profile at 1 chord length downstream of the airfoil

Figure 7 is the comparison of vortex field downstream of the flapping airfoil between experiment and simulation of a similar case[5]. Figure 7(a) is a photo taken during the experiment. The flow visualization was implemented using glycol smoke. Figure 7(b) is the vorticity contours from the simulation results. The agreement is reasonably good, and both visualizations show a similar vortex shedding pattern.


(a)
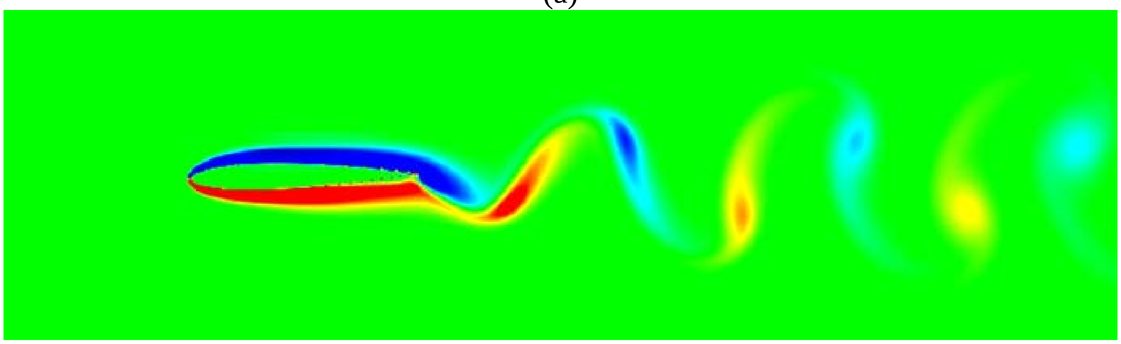
(b)
Figure 7, flow visualization comparison (a) experiment; (b) simulation

4. Conclusions

An airfoil flapping mechanism was designed, fabricated and implemented in wind tunnel tests. The test results agreed well with literature data. The low velocity in the bottom half of the test section was due to the presence of the linkage supporting the airfoil that blocks the flow. The results showed that flapping airfoil produced less drag comparing to stationary airfoil. Downstream velocity oscillation patterns were also different between the flapping airfoil and stationary airfoil, indicating different vortex shedding patterns in the downstream of the airfoil. The natural vortex shedding frequency of the stationary airfoil was dominated by the flapping frequency for the flapping airfoil case.

References

1. Mueller, T. J., “Aerodynamic Measurements at Low Reynolds Numbers for Fixed Wing Micro Aerial Vehicles”, RTO AVT/VKI Special Course on Development and Operation of UAVs for Military and Civil Applications, VKI, Belgium, September 13-17, 1999.
2. Free Online Private Pilot Ground School http://www.free-online-private-pilot-ground-school.com/aerodynamics.html
3. Ohmi, K., Coutanceau, M., Loc, T.P., and Dulieu, A. (1990). Vortex formation around an oscillating and translating airfoil at large incidences. J. Fluid Mech. 211**,** 37-60.

4. Zhang, N. and Zheng, Z.C., 2007, “An Improved Direct-Forcing Immersed-Boundary Method for Finite Difference Applications”, *Journal of Computational Physics*, 221 (1), 250-268
5. Zheng, Z. C., Zhang, N., Z, and Wei, Z., 2009, “Low-Reynolds Number Simulation for Flow over a Flapping Wing: Comparisons to Measurement Data” (invited), *Proc., 39th AIAA Fluid Dynamics Conference, June 22-25, 2009, San Antonio, TX*